RESULTS AND DISCUSSION

Influence of pH on the [Hb]/[Lipid] and metHb formation in the HbV

The pH of the Hb solution ([PLP] = 18 mM, [Hcy] = 10 mM) was adjusted from 6.8 to 7.4 with sodium carbonate at 37°C, and then HbVs were prepared. The resulting HbVs had various pHs in their inner aqueous phases. The [Hb]/[Lipid] of the resulting HbV showed that the maximum value was 1.8 at pH 7.0 (Fig. 1), relating to the isoelectric point (p*I* = 7.02, 25°C). In the pH of the Hb solution higher than the p*I*, the ξ- potential of Hb is negative, and the [Hb]/[Lipid] decreased because of the electrostatic repulsion between Hb molecules and the surface of the bilayer membrane. The pH of the Hb solution lower than the p*I* reduces the negative surface potential of the bimolecular membrane, resulting in the increased number of bilayer membranes. This is due to the low electrostatic repulsion between bilayer membranes of the lamellar structure of the lipid hydrate [4]. On the other hand, the metHb formation rate was suppressed in the higher pH because of the suppression of the proton oxidation, however, the higher pH increased the oxygen affinity higher than the value of RBC (P_{50}: 27 Torr).

Therefore, the pH value of the Hb solution should be adjusted to 7.0 during the preparation of HbV, and it is more desirable for the pH value to be adjusted to 7.4 where HbV functions as an oxygen carrier.

pH measurement of the inner aqueous phase of pyranine encapsulated vesicle

Pyranine is a sensitive and convenient probe to measure the pH of the aqueous solution. Figure 2 is the fluorescence spectra of pyranine in aqueous solutions with various pHs. The peaks at 365 nm and 405 nm appear at pH 5.3, and they decrease with increasing pH. However, the peak at 455 nm increases. Therefore, the ratio of fluorescent intensity at 455 nm to that at 405 nm can be used as a parameter which indicates the pH of the solution. The calibration curve of the ratio against the pH value obtained by a pH meter was linear in the pH region from 4 to 8.

We used the pyranine molecule as a pH probe of the inner aqueous phase of the vesicle, and encapsulated 0.5 mM of pyranine in the vesicle. When the pH of the outer aqueous phase was decreased from 7.3 to 5.8 by the addition of HCl, the pH of the inner aqueous phase decreased only from 7.3 to 6.9. This is because ion permeability through the bilayer membrane is too low (i.e, permeability of Cl^- is about 10^{-11} cm/s) [6].

On the other hand, when the CO_2 was dissolved into the pyranine encapsulating vesicle, the pH of the inner aqueous phase decreased with increasing partial pressure of CO_2. The pH change in the inner aqueous phase was in good agreement with the pH change of the outer aqueous phase which was measured by a pH meter (Fig. 3). Therefore, we confirmed that the pH of the inner aqueous phase could be controlled by changing the partial pressure of CO_2.

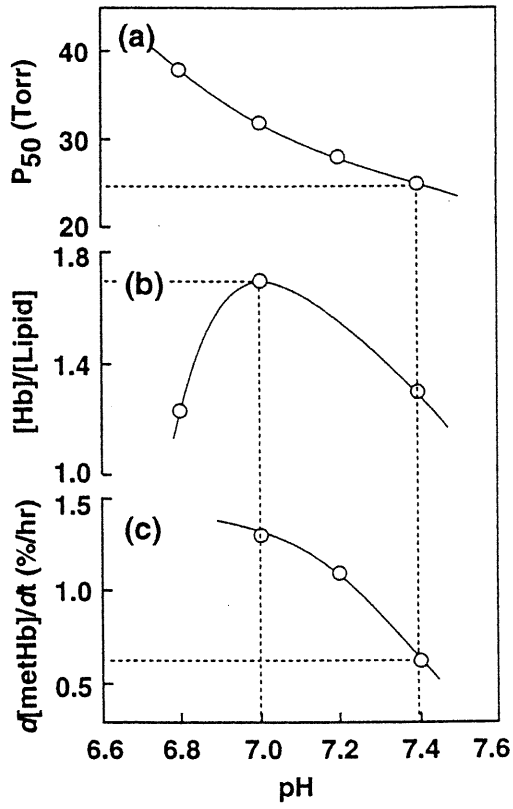

FIGURE 1 Influence of pH of the Hb solution on (a) P_{50} of the HbV, (b) [Hb]/[Lipid] ratio of the HbV, and (c) metHb formation rate of the HbV.

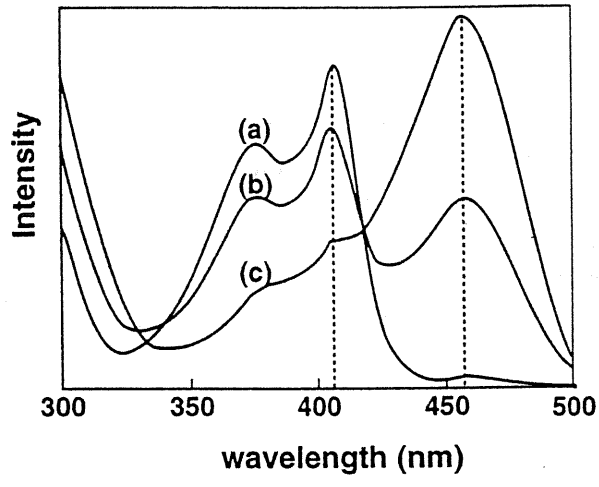

FIGURE 2 Excitation spectra of pyranine in aqueous buffer solutions at (a) pH 5.3, (b) pH 7.0, (c) and pH 7.8 at 25°C. ([pyranine] = 1 μM, λ_{em} = 510 nm)

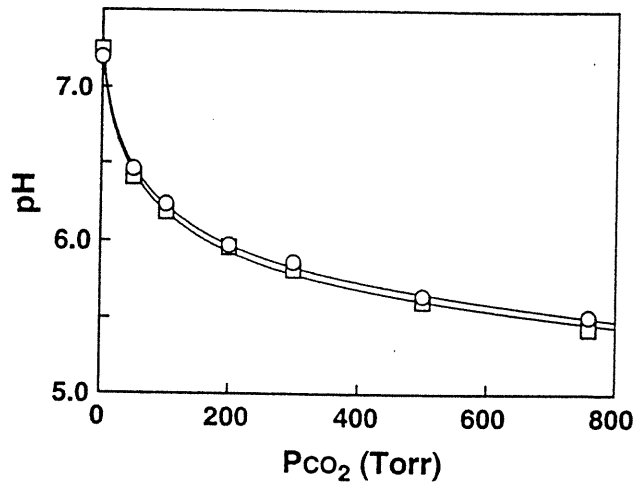

FIGURE 3 Influence of P_{CO_2} on pH in the inner and the outer aqueous phases of the vesicle. ([pyranine] = 1 μM in pH 7.3 phosphate buffer saline): (○) the inner phase pH calculated by the calibration curve, (□) the outer phase pH which measured by a pH electrode.

pH-control of the Hb solution by CO_2 gas

In accordance with Henry's law, under the constant temperature and constant partial pressure of CO_2, the volume of the CO_2, which was dissolved in the pure water, was theoretically calculated. The pH value of pure water or a saline solution which has no buffer effect at 37°C can be expressed in equation (1).

$$pH = 4.9\text{-}0.5 \log(P_{CO_2}) \quad (1)$$

Hemoglobin has a buffer effect against the pH change. Therefore, in the case of the Hb solutions, the relationship between pH and P_{CO_2} should be influenced by the concentration of the Hb solution at constant temperature as shown in Fig. 4 (a), and could be expressed in equation (2) at 37°C.

$$pH = 7.94 + 0.36 \log[Hb] - (0.856\text{-}0.148 \log[Hb])\log(P_{CO_2}) \quad (2)$$

On the other hand, under the constant concentration of the Hb solution is 38 g/dL, the relationship between the pH and the P_{CO_2} could be expressed in equation (3) using temperature (t°C) as shown in Fig. 4 (b).

$$pH = (20.4\text{-}0.025t) - (0.85\text{-}0.005t)\log(P_{CO_2}) \quad (3)$$

Characteristics of pH-controlled HbV by using CO_2 gas

At a constant concentration of the Hb solution (38 g/dL) and constant temperature (37°C), the value of the partial pressure of CO_2 was calculated using

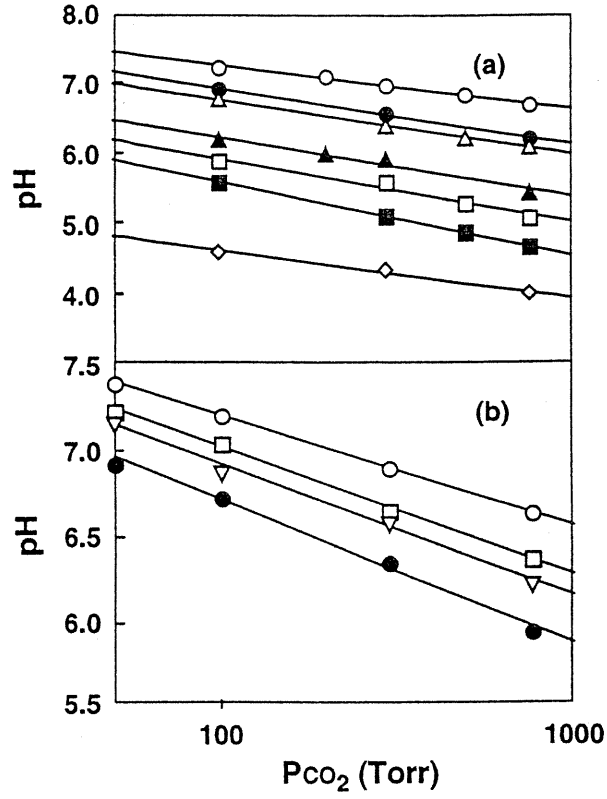

FIGURE 4 (a) Influence of P_{CO_2} on pH in the various Hb concentrations at 37°C: (○) [Hb]=40 g/dL, (●) [Hb]=10 g/dL, (△) [Hb]=5 g/dL, (▲) [Hb]=1 g/dL, (□) [Hb]=0.4 g/dL, (■) [Hb]=0.1 g/dL, (◇) saline.
(b) Influence of P_{CO_2} on pH in various temperatures at [Hb]=38 g/dL: (○) at 37°C, (□) at 26°C, (▽) at 18°C, (●) at 4°C.

equations (2) and (3), which are used for adjusting the pH of the Hb to 7.0. HbV was prepared the using CO_2 gas that dissolving the CO_2/N_2 mixed gas (P_{CO_2} = 130 Torr) into the Hb solution, and the pH was adjusted to 7.0 at 37°C. After an extrusion procedure, the solution pH was adjusted to 7.4 by reducing the pressure, which was confirmed by a pH meter. Table 1 shows the characteristics of the HbVs. The [Hb]/[Lipid] of the HbV, which was prepared using CO_2 gas, was 1.7, and it was higher than that (1.3) prepared at pH 7.4. The oxygen affinity (P_{50}) of the pH-controlled HbV using CO_2 gas was 25 Torr, and it was almost the same value as HbV prepared from the Hb solution with pH 7.4. Figure 5 shows the metHb formation of HbV of which inner aqueous phase was pH 7.4 and 7.0 at an

TABLE 1. Characteristics of HbVs

parameter	the inner aqueous phase pH		
	7.4 (CO_2 control)	7.4	7.0
diameter (nm)	266±90	243±71	261±80
[Hb] (g/dL)	10.0	10.0	10.0
[Hb]/[Lipid]	1.7	1.3	1.8
[metHb] (%)	3.0	2.2	2.4
P_{50} (Torr)	25	24	32
OTE (%)	28	27	35
Hill number	2.0	2.0	2.1
the outer aqueous pH (37°C)	7.4	7.4	7.4

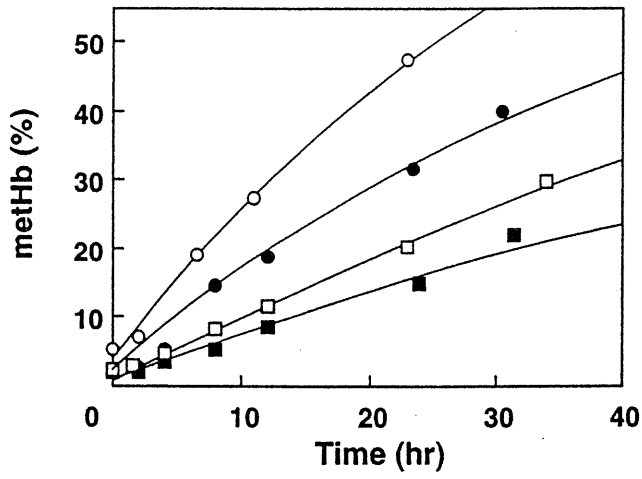

FIGURE 5 Time course of metHb formation in HbV dispersions at 37°C. In P_{O_2} of 149 Torr; (□) pH 7.0, (■) pH 7.4. In P_{O_2} of 23 Torr; (○) pH 7.0, (●) pH 7.4.

the oxygen partial pressure of 23 Torr and 149 Torr. The rate of metHb formation under the P_{O_2} of 23 Torr was always higher than that under the P_{O_2} of 149 Torr. It was reported that the rate of metHb formation increased with decreasing P_{O_2}, because the deoxyHb, to which H_2O was weakly coordinated, reacted with oxygen to form metHb more rapidly than did HbO_2. The maximum rate of metHb formation was at a P_{O_2} of 23 Torr [9,11].

At both oxygen partial pressures, the metHb formation was suppressed in the pH-controlled HbV using CO_2 gas, and then the metHb formation rate was only about 60% of the HbV which had an Hb of pH 7.0 because of the suppression of the proton oxidation.

Therefore, it is strongly expected that the pH-controlled HbV by CO_2 gas, which has a high [Hb]/[Lipid] value and a low rate of metHb formation, should work as an good oxygen carrier.

CONCLUSION

The pH of the inner aqueous phase of vesicle was measured by pyranine, and we confirmed that the pH of the inner aqueous phase of HbV could be controlled by the changing the partial pressure of CO_2. The pH-controlled HbV by CO_2 gas showed the high [Hb]/[Lipid] value of 1.7 with a low rate of metHb formation.

ACKNOWLEDGEMENTS

This work was partially supported by the project of Materials Research Laboratory for Bioscience and Photonics in Waseda University, Health Science Research Grant (Artificial Blood Project) from the Ministry of Hearth and Welfare, Japan, Grants-in-Aid from the Ministry of Education, Science, and Culture, Japan (08680940), and Kawakami Memorial Foundation.

REFERENCES

1. Djordjevich, J., Mayoral, I.F. and Ivankovich, A.D. Cardiorespiratory effect of exchange transfusions with synthetic erythrocytes in rats. *Crit. Care Med.*, **15**, 318-323 (1987).

2. Rudolph, A.S. Encapsulation of hemoglobin in liposomes, in *Blood Substitute: Physiological Basis of Efficacy*, Winslow, R.M., Vandegriff, K.D. and Intaglietta, M. (eds.), Birkhäuser, Boston, 1995, pp.90-104.

3. Tsuchida, E. and Takeoka, S. Stabilized hemoglobin vesicles, in *Artificial Red Cells*, Tsuchida, E. (ed.), Wiley, New York, 1995, pp.35-64.

4. Takeoka, S., Ohgushi, T., Terase, K., Ohmori, T. and Tsuchida E. Layer-controlled hemoglobin vesicles by interaction of hemoglobin with a phospholipid assembly. *Langmuir*, **12**, 1755-1759 (1996).

5. Nichols, J.W., Hill, M.W., Bangham, A.D. and Deamer, D.W. Measurement of net proton-hydroxyl permeability of large unilamellar liposome with the fluorescent pH probe, 9-amino-acridine. *Biochim. Biophys. Acta*, **596**, 393-403 (1980).

6. Albert, B., Bray, D., Lewis, J., Raff, M., Roberts, K. and Watson, J.D. (ed.) *Molecular Biology of the Cell*, Garland Publishing Inc., 1983, pp.287.

7. Kano, K. and Fendler, J.H. Pyranine as a sensitive pH probe for liposome interiors and surface. *Biochim. Biophys. Acta*, **509**, 289-299 (1978).

8. Clement, N.R. and Gould, J.M. Pyranine (8-Hydroxy-1,3,6-pyrenetrisulfonate) as a probe of internal aqueous hydrogen ion concentration in phospholipid vesicles. *Biochemistry*, **20**, 1534-1538 (1981).

9. Takeoka, S., Sakai, H., Kose, T., Mano, Y., Seino, Y., Nishide, H. and Tsuchida, E. Methemoglobin formation in hemoglobin vesicles and reduction by encapsulated thiols. *Bioconjugate Chem.*, **8**, 539-544 (1997).

10. Chung, J.E., Hamada, K., Sakai, H., Takeoka, S. and Tsuchida, E. Ligand exchange reaction of carbonylhemoglobin to oxihemoglobin in a hemoglobin liquid membrane., *Nihonkagakukaishi*, **2**, 123-127 (1995).

11. Brantley, R.E., Smerdon, S.J., Wilkinson, A.J., Singleton, E.W. and Olson, J.S. The mechanism of autoxidation of myoglobin, J. Biol. Chem. 268, 6995-7010 (1993)

ART. CELLS, BLOOD SUBS., AND IMMOB. BIOTECH., 26(5&6), 507-517 (1998)

OXYGEN RELEASING FROM CELLULAR HEMOGLOBIN

Noriyuki Kawai, Haruki Ohkawa, Hiromitsu Maejima, Shinji Takeoka,
Hiroyuki Nishide, and Eishun Tsuchida*
Department of Polymer Chemistry, ARISE,
Waseda University, Tokyo 169-8555, Japan

Abstract: The oxygen-releasing behavior of hemoglobin vesicles (HbV) was measured in order to study the difference in oxygen dynamics inside and outside the cellular Hb using a conventional stopped flow method and a newly developed stopped flow flash photolysis method. The partial pressure of oxygen in the solution outside the HbV was monitored with the lifetime of the triplet state of meso-tetraphenylporphinatozinc(II) bound to human serum albumin excited by the laser flash. The change in the partial pressure of oxygen outside the HbV showed a biphasic profile and was slower than that inside the HbV. The first phase shows the oxygen- releasing process from Hb near the phospholipid bilayer membrane, and the second phase is considered the process in which oxygen diffuses to the bulk aqueous region and reaches the equilibrium value.

INTRODUCTION

Hemoglobin (Hb)-based oxygen carriers can be structurally classified into two groups; one is acellular Hbs, and the other is cellular Hbs. Acellular Hbs are modified Hbs such as intramolecularly crosslinked Hbs, intermolecularly crosslinked Hbs, and polymer-conjugated Hbs [1]. Some acellular Hb solutions are now in the final stage (phase III) of clinical trials [2]. However, several issues have been pointed out regarding acellular Hbs. Especially, the high affinity of acellular Hb for nitric oxide induces injected Hb to act as an endothelium- derived relaxing factor (EDRF), leading to vasoconstriction and then elevation of blood pressure [3]. Furthermore, the generation of oxidants facilitated by Hb, the

*To whom all the correspondence should be addressed.

toxicity of Hb metabolites, the enhancement of Hb toxicity by complexation with endotoxin, the change in microcirculation caused by the difference in the oxygen transporting properties and the solution properties, etc., have often been discussed [4, 5]. On the other hand, HbV is one kind of cellular Hbs which encapsulates concentrated Hb with the phospholipid bimolecular membrane. The advantage of the cellular Hbs is that the particle size, the thickness of the membrane, the Hb concentration inside the cell, the solution viscosity, and the oxygen affinity are controllable [6, 7]. It is noted that the size difference of acellular Hb (ca. 5 nm), cellular Hb (ca. 250 nm) and red blood cells (ca. 8000 nm) causes different solution viscosity, capillary permeability, oxygen dynamics, etc., and the biological activity or toxicity attributed to Hb is suppressed by Hb encapsulation. Especially, the difference in the oxygen-binding and releasing kinetics of oxygen carriers from RBC would result in a change in the tissue distribution of oxygen density after the injection of oxygen carriers in spite of the similar oxygen-binding and dissociation equilibrium curves [8, 9]. Therefore, it is necessary to measure precisely the oxygen-binding and releasing kinetics of oxygen carriers in *in vitro* controlled systems to collect the basic data.

The laser flash photolysis method (LFP) [10] and the stopped flow method (SF) [11] have been used conventionally to measure oxygen dynamics. LFP is a method of measuring the binding and dissociation kinetics (k_{on}, k_{off}) of various ligands. In this case, the oxygen dynamics around the oxygen binding site (Hb) can be observed, and in the case of cellular Hbs, the oxygen diffusion process toward the outside the cell should not be included. On the other hand, SF is a method of analyzing the oxygen dynamics of Hb, relating to the oxygen diffusion process at the inside and the outside the cell, because a UV-Vis. spectral change is initiated after the rapid mixing of two solutions (e.g., one is the solution of oxygen carriers, and the other is the deoxygenated $Na_2S_2O_4$ solution [12]). In this case, the change in the absorption of the heme moiety accompanied by oxygen coordination to Hb can be measured, representing the oxygen dynamics inside the cell. It is important to analyze the oxygen dynamics outside cellular Hb as well as inside because oxygen transport by cellular Hb should be carried out from Hb in the cell to the plasma and/or tissue regions.

In recent years, a series of new metalloporphyrin derivatives has been exploited to measure oxygen partial pressure using the quenching phenomena of the excited state by oxygen [13, 14]. The lifetime of the excited state induced by laser flash is influenced by the oxygen concentration in the solution. This method is better for analyzing the oxygen dynamics on a millisecond scale in comparison with the method using an oxygen polarographic electrode on a second scale.

We aimed to compare the oxygen dynamics of oxygen carriers such as acellular and cellular Hbs, using a newly developed method, stopped flow flash photolysis, which combined SF with LFP. In this paper, the oxygen releasing kinetics from HbV is monitored by the oxygen probe compared to that in the HbV.

MATERIALS AND METHODS

Materials Hb vesicles (HbV) [15, 16] and intramolecular crosslinked Hb (XLHb) [17] were prepared in the same way as previously reported. Pyridoxal 5'-phosphate was used as an allosteric effector. *Meso*-tetraphenylporphinatozinc (II) (ZnTPP) binding to human serum albumin (HSA) was prepared as follows. A dimethylsulfoxide solution of ZnTPP ([ZnTPP]: $2x10^{-4}$ mol L^{-1}) was added to an HSA aqueous solution ([HSA]= 0.7 wt%) and stirred for about 30 min. Dimethylsulfoxide was removed by ultrafiltration (cutoff: 50 kD) and dialyzed against saline to obtain a transparent reddish purple solution ([ZnTPP]: $7.5 x10^{-4}$ mol L^{-1}).

Measurements of solution properties The oxygen-binding and dissociation equilibrium curves of oxygen carriers were obtained with a Hemox Analyzer (TCS Medical Products) at pH 7.4, 37 °C. The solution viscosity of the oxygen carriers was measured with a dynamic capillary rheometer (OCR-D, Anton Paar). A submicron particle analyzer (N4 SD, Coulter) was used to measure the size and size distribution of HbV.

Stopped flow method Oxygen dynamics was measured using a stopped flow apparatus (model TSP-601, Unisoku). For the measurement of oxygen dissociation, equal volumes ($1.25x10^{-4}$ L) of an oxygen carrier solution ([heme]: $2x10^{-5}$ mol L^{-1}) at a partial pressure of oxygen (Po_2) of 37 Torr and a phosphate buffered solution in a nitrogen atmosphere were rapidly mixed in a mixing cell at 37 ± 0.2 °C. The oxygen dissociation was monitored at 415 nm (oxy Hb) and 430 nm (deoxy Hb). A xenon lamp (150 W) was used as a monitor light source equipped with a cutoff filter (type L-39, Hoya) to eliminate the light in the ultraviolet region.

Stopped flow flash photolysis method The Po_2 in the solution outside the oxygen carriers was determined by time-resolved stopped flow spectroscopy attached to the flash photolysis apparatus (model TSP-601, Unisoku) (Figure 1). The relationship between the decay of the excited triplet state (k_T) of the porphinatozinc(II) bound to HSA and the Po_2 in the solution was obtained as follows. The oxygen probe solution ([ZnTPP]: $1.0x10^{-4}$ mol L^{-1}, before mixing) and the phosphate buffered saline were put into each reservoir tank of the stopped flow mixer and saturated with various Po_2 (0-80 Torr). After the rapid mixing of these two solutions (dead time: < 1 ms), the mixture was irradiated with a Nd-YAG laser pulse (532 nm), and the k_T value was obtained by the triplet-triplet absorption change at 470 nm. k_T and Po_2 were plotted and fitted by the method of least squares.

For the measurement of the oxygen dissociation reaction, equal volumes (1.25×10^{-4} L) of the oxygen carrier solution ([heme]: 4×10^{-5} mol L^{-1}, Po_2: 37 Torr) and a phosphate buffered solution containing the oxygen probe ([ZnTPP]: 1.0×10^{-4} mol L^{-1}) in a nitrogen atmosphere were rapidly mixed in a mixing cell, and a laser pulse was irradiated after some delay times (1-5000 ms) from rapid mixing. k_T was obtained by monitoring the triplet-triplet absorption change at 470 nm. Po_2 in the mixed solution was calculated from the equation for k_T-Po_2 .

RESULTS AND DISCUSSION

Solution properties Table 1 summarizes the properties of oxygen carriers used in this experiment. XLHb is acellular Hb of which the α subunits are crosslinked not to dissociate into $\alpha\beta$ dimers in a diluted solution ($<1 \times 10^{-4}$ mol L^{-1}). The HbV encapsulating concentrated Hb (ca. 38 g dL^{-1}) with a mixed phospholipid bilayer membrane was used as cellular Hb. The size of HbV was controlled to 251 ± 69 nm by passing the dispersion through the 0.22 $\mu m\phi$ isopores of the membrane filter by an extrusion method. The viscosities of the XLHb, HbV, and RBC solutions (pH 7.4, 37 °C, [Hb]: 10 g dL^{-1}) were 1.0, 3.6, and 4.0 cP, respectively.

The P_{50} of XLHb (31 Torr) was larger than that of the stroma-free Hb (9 Torr), because the crosslinking reagent reacted with deoxyHb and stabilized its quaternary structure as a T-state. The P_{50} of HbV can be controlled by the kind of coencapsulated allosteric effectors and their concentration. Figure 2 shows the oxygen binding and dissociation equilibrium curves of these oxygen carriers. P_{50} of the HbV was controlled to 19 and 33 Torr by coencapsulating 1-fold and 3-fold pyridoxal 5'-phosphate of Hb in molar ratio, respectively.

The surface area and the volume of oxygen carriers are shown in Table 1. The surface area and volume of one particle become larger with increasing particle size. In the case of the total surface area (A_T) of particles in the solution with the same concentration of Hb the A_T of red blood cell is assumed to be 1, that of HbV is about 13, and that of XLHb is 670. The A_T is an important factor for the oxygen kinetics, because A_T indicates the interface of oxygen transfer from the oxygen carriers to the outer aqueous phase.

Measurement of oxygen concentration The lifetime of the excited state of HSA-ZnTPP induced by the laser flash was proportional to the oxygen pressure in the solution in the range from 0 to 80 Torr (equation : $k_T = 331 \times Po_2 + 951$). It was confirmed that HSA-ZnTPP can function effectively as a probe to determine the oxygen concentration in the solution. In recent years, methods of determining oxygen concentration utilize the phosphorescence lifetime of excited porphyrin

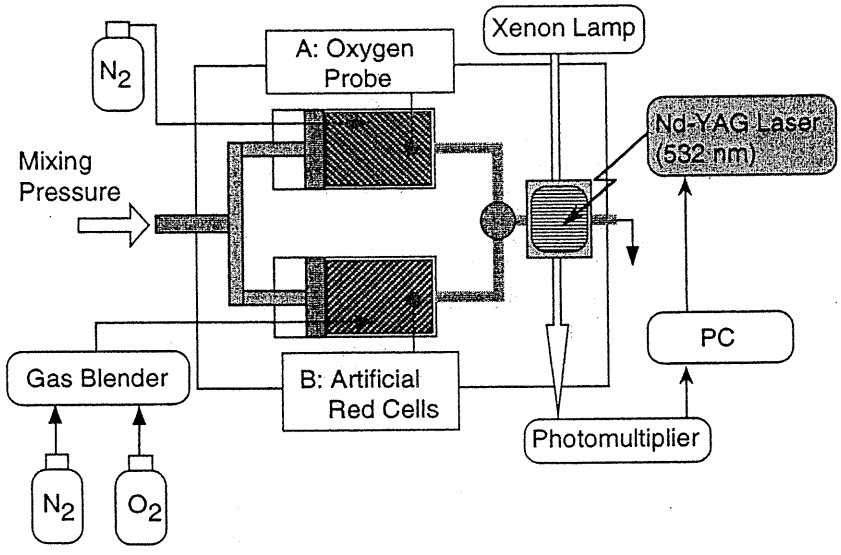

FIGURE 1 Stopped flow flash photolysis apparatus.

molecules [13]. A series of new palladium porphyrin derivatives bound to bovine serum albumin has been used as oxygen probes, and the phosphorescence decay after the laser flash was monitored to measure the oxygen concentration. Usually, several hundred times accumulation was carried out to obtain the lifetime with a good decay curve because of the low phosphorescence intensity [14]. However, in our method, because the reaction initiated by rapid mixing of two solutions is monitored, it is not suitable for multiple accumulations. A porphinatozinc(II) derivative having a relatively large triplet-triplet absorption change was then selected as an oxygen probe, and the Po_2 was calculated from the lifetime of the excited triplet state over an accumulation of 64-128 times.

Oxygen-releasing dynamics In Figure 3, the oxygen-releasing process from the acellular XLHb (P_{50}=31 Torr) obtained by the SFFP method was shown. This reaction was initiated by mixing equal volumes of the XLHb solution ([heme]: $4x10^{-5}$ mol L^{-1}) at a Po_2 of 37 Torr and a deoxygenated phosphate buffered solution containing the oxygen probe ([ZnTPP]=$1.0x10^{-4}$ mol L^{-1}) in a nitrogen atmosphere. The Po_2 in the solution just after mixing (1 ms) was half of the value (Po_2=18.5 Torr) before mixing. The oxygen concentration in the solution was simply increased and reached an equilibrium value (22.4 Torr) within 200 ms. This concentration was in good agreement with the value that had been calculated from the oxygen-binding equilibrium curve (Figure 2); that is, the oxygen

Table 1 Characterization of oxygen carriers

Samples	XLHb	HbV1	HbV2	Red Blood Cells
Paricle diameter (nm)	5	238±66	254±83	8000
P_{50} (Torr)	31	19	33	27
Hill number (-)	1.8	1.5	1.9	2.8
Volume of 1 particle (μm^3)	6.5×10^{-8}	7.1×10^{-3}	8.6×10^{-3}	90
Surface area of 1 particle (μm^2)	7.8×10^{-5}	0.18	0.2	160
Ratio of total surface area (-)	670	14	13	1

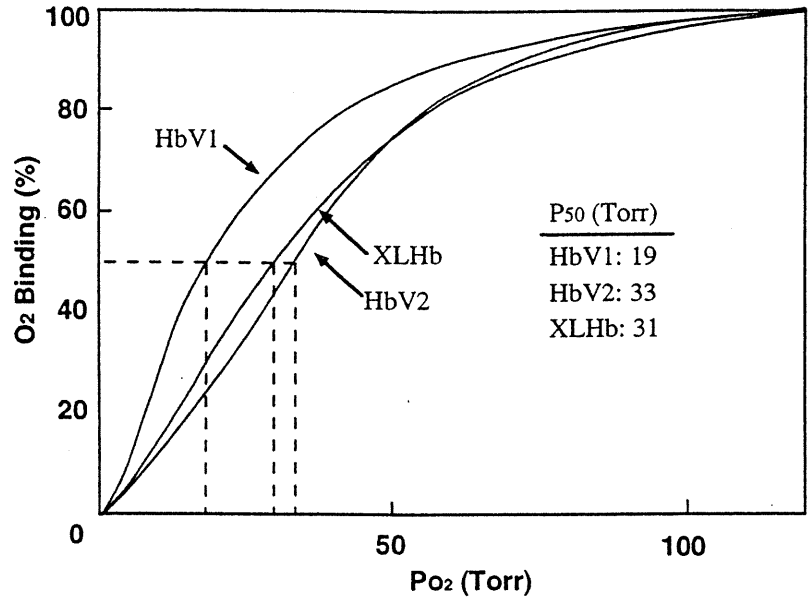

FIGURE 2 Oxygen-binding and dissociation equilibrium curves of oxygen carriers. Phosphate buffer solution, pH 7.4, 37 °C.

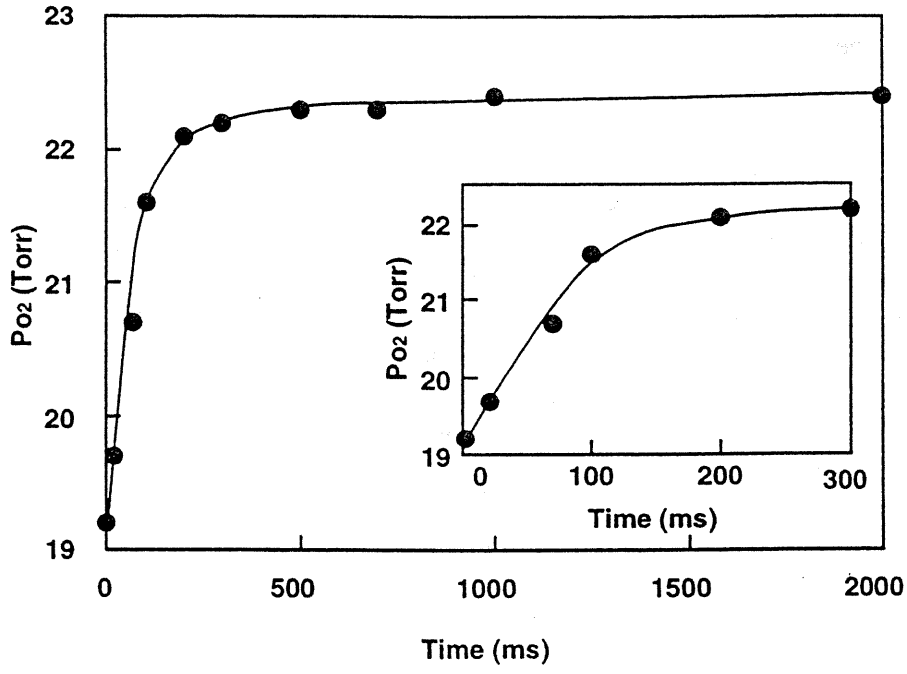

FIGURE 3 Oxygen releasing kinetics of XLHb measured by the SFFP method. XLHb solution; [Hb]=4x10^{-5} mol L^{-1}, Po_2=38.2 Torr. Probe solution: [ZnTPP] =1x10^{-4} mol L^{-1}, Po_2=0 Torr (before mixing). In phosphate buffer solution, pH 7.4, 37 °C. Monitored at 470 nm. Detailed initial change is inserted in the figure.

concentration reached a new equilibrium point after mixing of equal volumes of the XLHb solution equilibrated at a Po_2 of 37 Torr and the deoxygenated buffer solution. The apparent rate constant of oxygen release (k_{off}) from XLHb (17 s^{-1}) was calculated from the initial change in the oxygen concentration and showed good agreement with the value measured by the SF method (28 s^{-1}) [18]. Therefore, the SFFP method was confirmed to be a useful method of determining the oxygen dynamics of oxygen carriers.

Figure 4(a) shows the change in the Po_2 of the outer aqueous phase with the HbV after the equal volume mixing of the HbV solution in an equilibrium state (Po_2: 37.0 Torr) with the completely deoxygenated buffer solution of the oxygen probe ([ZnTPP]= $1x10^{-4}$ mol L^{-1}, pH 7.4, 37 °C). Two phases were observed in this change: the first phase was the fast phase within ca. 100 ms, and the second phase was the slow phase up to *ca.* 1000 ms. In the case of HbV1, the Po_2 increased from 18.5 to 20.9 Torr and finally reached an equilibrated value of 21.8 Torr within 1000 ms. The change was converted to the change in the percentage of the oxygenation saturation using the oxygen binding and dissociation equilibrium curve shown in Fig. 2. 5.2 % of the bound oxygen in the HbV was released in the first phase; then 1.2% was released in the second phase. Therefore, a total of 6.4 % was released from HbV. The Po_2 in the solution of HbV2 reached an equilibrated value of 22.3 Torr. This value was higher than that of HbV1, because the P_{50} of HbV2 (33 Torr) was higher than that of HbV1 (19 Torr). And, these equilibrated values matched those values calculated from OEC.

The change in oxygen saturation (So_2) of Hb in the HbV was observed using the SF method under the same conditions as that of SFFP in Figure 4(a). As shown in Figure 4(b), the change in the So_2 of Hb did not show a biphasic profile as the change in a Po_2 from the SFFP method. Within 60 ms after mixing, the percentage of So_2 changed to 85% of the value that was estimated to be equilibrated under these conditions and almost reached the equilibrated value (58 %) within 1000 ms. This value was in good agreement with the percentage (57 %) of So_2 of Hb obtained from the SFFP method (Figure 4(a)). In the case of HbV (P_{50}= 19 Torr) in Figure 4(a), the percentage of So_2 still remained at 50% of the value that was estimated to be equilibrated at 60 ms after mixing. Therefore, for the Po2 in the outer aqueous phase of HbV measured by the SFFP method and the percentage of So_2 in HbV obtained by the SF method, the equilibrated values showed good correspondence; however, their kinetics on changing to the equilibrium value indicated a significant difference. That is, the change obtained from the SF method (inside) was faster than that from the SFFP method (outside).

The first phase shows the oxygen-releasing process from Hb near the phospholipid bilayer membrane, and the second phase is considered to be the process in which oxygen diffuses to the bulk aqueous region and reaches the

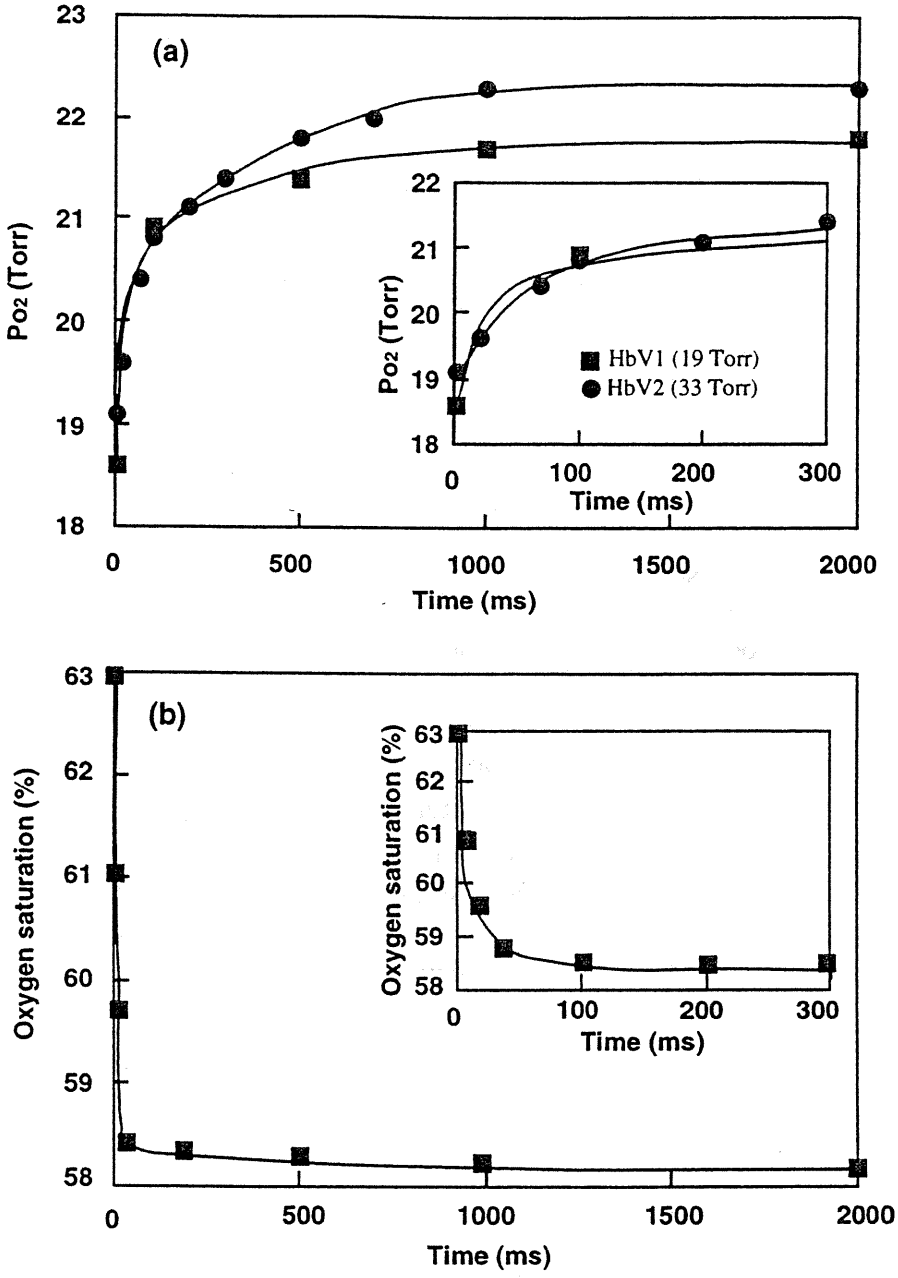

FIGURE 4 Oxygen releasing kinetics of HbV measured by the SFFP (a) and the SF (b) method. HbV1 (P_{50}=19 Torr); Po_2=37.0 Torr, HbV2 (P_{50}=33 Torr); Po_2=38.2 Torr, [Hb]=4x10^{-5} mol L^{-1} (before mixing). Phosphate buffer solution (pH 7.4, 37 °C). (a) Sample: HbV1 and HbV2. Probe solution: [ZnTPP]=1x10^{-4} mol L^{-1}, Po_2=0 Torr. Monitored at 470 nm. (b) Sample: HbV1. Buffer solution: Po_2=0 Torr. Monitored at 432 nm.

equilibrium value. The latter process should give an averaged value for the bulk phase with delay time because the oxygen probes existed homogeneously in the outer aqueous solution. It is concluded that the oxygen diffusion from near the bilayer to the bulk phase causes the delay time of the oxygen concentration change compared with the change inside the HbV.

In this paper, we could not show results with red blood cells under the same conditions because hemolysis occurred when the red blood cells passed through the rapid mixer. It is assumed that an unstirred layer of solvent adjacent to the cell surface would influence the diffusion of the released oxygen, and the unstirred layer increases following the particle size of the oxygen carrier would become larger [19]. The delay time of the oxygen concentration change would then be more remarkable in the case of red blood cells.

ACKNOWLEDGEMENT

This work was partially supported by the project of Material Research Laboratory for BioScience and Photonics in Waseda University and Health Science Research Grants (Artificial Blood Project) from the Ministry of Health and Welfare, Japan.

References

1. Chang, T.M.S. Present Status and Future Perspectives of Modified Hemoglobin as Red Blood Cell Substitutes *in* Artificial red cells. Tsuchida, E. (ed), John Wiley & Sons, New York, 21-34 (1995).
2. Farmer, M.C. Przybelski, R.J., McKenzie, J.E., Burhop, K.E. Preclinical Data and Clinical Trials with Diaspirin Cross-linked Hemoglobin *in* Artificial red cells. Tsuchida, E. (ed), John Wiley & Sons, New York, 177-186 (1995).
3. Motterlini, R. Interaction of Hemoglobin with Nitric Oxide and Carbon Monoxide: Physiological Implications *in* Blood Substitutes: New Challenges. Winslow, R.M., Vandegriff, K.D., Intaglietta M. (eds), Birkhauser, Boston, 74-98 (1995).
4. Tsuchida, E. (ed) Artificial red cells, John Wiley & Sons, New York (1995).
5. Winslow, R.M., Vandegriff, K.D., Intaglietta M. (eds) Blood Substitutes: New Challenges. Birkhauser, Boston (1995).
6. Djordjevich, L., Miller, I.F. Synthetic Erythrocytes from Lipid Encapsulated Hemoglobin. Exp Hemat **8**: 584-592 (1980).
7. Winslow, R.M., Vandegriff, K.D., Intaglietta M. (eds) Blood Substitutes: Physiological Basis of Efficacy. Birkhauser, Boston, 90-104 (1995).
8. Vandegriff, K.D., Intaglietta M. A Theoretical Analysis of Oxygen Transport: A New Strategy for the Design of Hemoglobin-based Red Cell

Substitutes *in* Blood Substitutes: Physiological Basis of Efficacy. Winslow, R.M., Vandegriff, K.D., Intaglietta M. (eds) Birkhauser, Boston, 143-154 (1995).

9. Tsai, A.G., Kerger, H., Intaglietta M. Microvascular Oxygen Distribution: Effects Due to Free Hemoglobin *in* Blood Substitutes: New Challenges. Winslow, R.M., Vandegriff, K.D., Intaglietta M. (eds), Birkhauser, Boston, 124-131 (1995).
10. Olson, J.S. Stopped-Flow, Rapid Mixing Measurements of Ligand Binding to Hemoglobin and Red Cells. Method *in* Enzymology 76: Hemoglobins. Academic Press Inc. New York, 631-651 (1981).
11. Mathews, A.J., Olson, J.S. Assignment of Rate Constants for O_2 and CO Binding to α and β Subunits within R- and T-State Human Hemoglobin. Method *in* Enzymology 232: Hemoglobins part C. Academic Press Inc. New York, 363-386 (1994).
12. Coin, J.T., Olson, J.C. The Rate of Oxygen Uptake by Human Red Blood Cells. J Biol Chem **254**: 1178-1190 (1979).
13. Vanderkooi, J.M., Maniara, G., Green, T.J., Wilson, D.F. An Optical Method for Measurement of Dioxygen Concentration Based upon Qunching of Phosphorescence. J Biol Chem **252**: 5476-5482 (1987).
14. Torres Filho, I.P., Intaglietta, M. Microvessel Po_2 Measurements by Phosphorescence Decay Method. Am J Physiol **265**: H1434-H1438 (1993).
15. Sakai, H., Takeoka, S., Park, S.I., Kose, T., Nishide, H., Izumi, Y., Yoshizu, A., Kobayashi, K., Tsuchida, E. Surface Modification of Hemoglobin Vesicles with Poly(ethyleneglycol) and Effects on Aggregation, Viscosity, and Blood Flow during 90% Transfusion in Anesthetized Rats. Bioconjugate Chem **8**: 23-30 (1997).
16. Takeoka, S., Ohgushi, T., Terase, K., Ohmori, T., Tsuchida, E. Layer Controlled Hemoglobin Vesicles by Interaction of Hemoglobin with Phospholipid Assembly. Langmuir **12**: 1775-1779 (1996).
17. Winslow, R.M., Chapman, K.W. Pilot-Scale Preparation of Hemoglobin Solutions. Method in Enzymology 231, Hemoglobins Part B. Academic Press Inc. New York, 3-16 (1994).
18. Vandegriff, K.D., Le Tellier, Y.C., Winslow, R.M., Rohlfs, R.J., Olson, J.S. Determination of the Rate and Equilibrium Constants for Oxygen and Carbon Monoxide Binding to R-state Human Hemoglobin Cross-linked between the α Subunits at Lysine 99. J Biol Chem **266**: 17049-17059 (1991).
19. Vandegriff, K.D., Olson, J.S. A Quantitative Description in Three Dimentions of Oxygen Uptake by Human Red Blood Cells. Biophys J **45**: 825-835 (1984).

ART. CELLS, BLOOD SUBS., AND IMMOB. BIOTECH., 26(5&6), 519-527 (1998)

HUMAN SERUM ALBUMIN-BOUND SYNTHETIC HEMES AS AN OXYGEN CARRIER: DETERMINATION OF EQUILIBRIUM CONSTANTS FOR HEME BINDING TO HOST ALBUMIN

Teruyuki Komatsu, Kazuyoshi Hamamatsu, Shinji Takeoka, Hiroyuki Nishide, Eishun Tsuchida[†,*]

Department of Polymer Chemistry, ARISE, Waseda University, Tokyo 169-8555, Japan
[†]CREST investigator, Japan Science and Technology Corporation

ABSTRACT

Human serum albumin (HSA) incorporating synthetic tetraphenylporphinato-iron(II) derivatives (FeP1 or FeP2) can bind and release oxygen reversibly under physiological conditions (in aqueous media, pH 7.4, 37°C). The maximal binding ratio of FeP1/HSA was estimated to be eight, and the stepwise equilibrium constants for FeP1 binding to HSA (K_1-K_8) ranged from 1.2×10^6 to 1.3×10^4 M^{-1}. The major binding sites of FeP1 are presumably identical to those of hemin, bilirubin and long-chain fatty acids. The O_2-binding ability of the HSA-FeP can be regulated by changing the molecular structure of the incorporated hemes. The half-lifetime of the O_2-coordinated FeP2 in HSA was significantly longer than that of HSA-FeP1.

INTRODUCTION

Human serum albumin (HSA) in blood plasma plays two major roles, (i) maintaining the colloidal osmotic pressure and (ii) transporting numerous

*To whom the correspondence should be addressed.

endogenous and exogenous compounds with unusual ligand-binding properties. Hemin released from hemoglobin is also transported to the liver by HSA for metabolic processing. The binding equilibria of porphyrin derivatives to albumin have therefore been studied over the last two decades [1-5]. One may expect some new functions of these albumin-porphyrin complexes, little interest has, however, been generated so far [6]. We have recently found that a synthetic hemes, 2-[8-{N-(2-methylimidazolyl)}-octanoyloxymethyl}-5,10,15,20-tetrakis (α,α,α,α-*o*-pivalamido)phenylporphinatoiron(II) (FeP1) is efficiently incorporated into the HSA molecule, providing a new type of hemoprotein (HSA-FeP1), which can bind and release oxygen reversibly under physiological conditions (in aqueous media, pH 7.4, 37°C) as does hemoglobin [7, 8]. The 5 wt% (0.75 mM) of HSA-FeP (FeP/HSA: 8) solution should deliver 3.4 mL/dL of oxygen during the circulation between the lungs (Po_2: 110 Torr) and the mixed venous system (Po_2: 40 Torr). This amount corresponds to *ca.* 60% of the O_2-transport of human blood (5.9 mL/dL). The solution properties of HSA-FeP1 satisfied the physiological needs; the specific gravity was 1.013-1.021, and the viscosity was almost the same as that of HSA (1.3 cP). Our present interest in this new O_2-transport albumin is its nano-structure. At which place in the HSA molecule is FeP bound? It has been elucidated that HSA has 3 homologue domains (I, II and III) with 9 loops formed by 17 disulfide linkages, and each domain is constructed of 2 subdomains (IA, IB, *etc.*) [9]. In contrast to the early conception of an oblate ellipsoid shape (140x40 Å), a recent study of the crystal structure of HSA reveals a heart-shaped molecule which can be approximated to an equilateral triangle with sides of 80 Å and a depth of 30 Å [10, 11]. In this paper, we report the stepwise equilibrium constants for FeP binding to HSA and the major binding sites of the FeP molecule. Furthermore, we describe that the half-lifetime of O_2-coordinated species can be controlled by changing the structure of FeP.

EXPERIMENTAL SECTION

Materials.

FeP1 and FeP2 were prepared according to our previously reported procedure [12, 13]. An HSA solution was purchased from Bayer Co., Ltd. (Albumin Cutter, 5 wt%). Protoporphyrin IX disodium salts (PPIX Na_2) was gifted from Sato Pharmacy Co., Ltd. Phenol red and palmitic acid were purchased from Kanto Chemical Co., Ltd. Pure water (Otsuka Pharmaceutical Co., Ltd.) was used for dilution of HSA and ethanol (purity; >99.5%, Kanto Chemical Co., Ltd.) or dimethylsulfoxide (special grade, Kanto Chemical Co., Ltd.) were for the solvent of FePs.

Preparation of HSA-FeP.

HSA-FeP solutions were prepared according to the previously reported procedure [8].